A reevaluation of the spleen tyrosine kinase (SYK) activation mechanism

Received for publication, February 15, 2019, and in revised form, March 25, 2019 Published, Papers in Press, March 28, 2019, DOI 10.1074/jbc.RA119.008045

My S. Mansueto[‡], Abigail Reens[‡1], Larissa Rakhilina[‡], An Chi[§], Bo-Sheng Pan[‡], and J. Richard Miller[‡2]

From the Departments of [‡]Pharmacology and [§]Chemical Biology, Merck & Co., Inc., Boston, Massachusetts 02115

Edited by Jeffrey E. Pessin

Spleen tyrosine kinase (SYK) is a signaling node in many immune pathways and comprises two tandem Src homology (SH) 2 domains, an SH2-kinase linker, and a C-terminal tyrosine kinase domain. Two prevalent models of SYK activation exist. The "OR-gate" model contends that SYK can be fully activated by phosphorylation or binding of its SH2 domains to a dual-phosphorylated immune-receptor tyrosine-based activation motif (ppITAM). An alternative model proposes that SYK activation requires ppITAM binding and phosphorylation of the SH2-kinase linker by a SRC family kinase such as LYN proto-oncogene, SRC family tyrosine kinase (LYN). To evaluate these two models, we generated directly comparable unphosphorylated (upSYK) and phosphorylated (pSYK) proteins with or without an N-terminal glutathione *S*-transferase (GST) tag, resulting in monomeric or obligatory dimeric SYK, respectively. We assessed the ability of a ppITAM peptide and LYN to activate these SYK proteins. The ppITAM peptide strongly activated GST-SYK but was less effective in activating upSYK untagged with GST. LYN alone activated untagged upSYK to a greater extent than did ppITAM, and inclusion of both proteins rapidly and fully activated upSYK. Using immunoblot and phosphoproteomic approaches, we correlated the kinetics and order of site-specific SYK phosphorylation. Our results are consistent with the alternative model, indicating that ppITAM binding primes SYK for rapid LYN-mediated phosphorylation of Tyr-352 and then Tyr-348 of the SH2-kinase linker, which facilitates activation loop phosphorylation and full SYK activation. This gradual activation mechanism may also explain how SYK maintains ligand-independent tonic signaling, important for B-cell development and survival.

SYK (spleen tyrosine kinase),[3] a cytoplasmic protein-tyrosine kinase (PTK), is crucial for mediating antigen-associated signals in various cell types of the innate and adaptive immune system (1, 2). This signal mediation is essential to the propagation and activation of hematopoietic cells such as B cells, mast cells, and platelets. Aggregation of IgE or ligand-binding receptors on the surface of the cells triggers the phosphorylation of immunoreceptor tyrosine-based activation motifs (ppITAMs) on the cytoplasmic tails of the CD79 heterodimer (B-cells), FcεRI (mast cells), and Fcγ (platelets). SYK is recruited by interaction with ppITAMs, and undergoes autophosphorylation (3–6) as well as phosphorylation by membrane-associated SRC kinases (7, 8). These phosphorylation events activate SYK, initiating multiple signaling cascades, which results in an array of inflammatory or immunological outcomes (9). SYK has also been implicated in tonic signaling, the ligand-independent stochastic activity mediated by pre-B cell and B cell receptors. This transient signaling is critical in directing and maintaining B cell development (10). Given its central role in mediating these biological responses, SYK has been pursued as a target for pharmacological modulation and treatment of autoimmune and inflammatory diseases as well as hematological cancers (11, 12). Fostamatinib, a nonselective inhibitor of SYK and the closely related kinase ZAP70 (13) was recently approved for treatment of chronic immune thrombocytopenia in patients with insufficient response to previous treatments.

The 72-kDa SYK protein consists of tandem N-terminal SH2 domains separated by an inter-SH2 domain (or interdomain A), and a C-terminal kinase domain. The tandem SH2 domains and the C-terminal kinase domain are separated by a region referred to as the interdomain linker (or interdomain B). Multiple phosphorylation sites are spread throughout the protein with a particularly high concentration in the interdomain linker (Fig. 1*A*). Recently, computational studies (14), cryo-EM (15), and high resolution X-ray structures of SYK and ZAP70 (16, 17) have provided insight into the similar unactivated/autoinhibited form of the kinases. One notable feature of the autoinhibited conformation is the formation of a linker-kinase sandwich, which brings the interdomain linker in proximity to the region between the two SH2 domains and the C-terminal helix of the kinase domain. This sandwich effect results in inactive SYK adopting a very compact structure that undergoes a transition to a more loosely-packed structure upon activation. In the autoinhibited state, SYK is minimally phosphorylated and exhibits a low level of kinase activity (16, 18). SYK can be autophosphorylated or phosphorylated by SRC family kinases at multiple nonequivalent phosphorylation sites across various domains of the protein, but it is also responsive to binding of ppITAM sequences in the cytoplasmic domain of immune receptor-associated proteins. This complex activation process may allow SYK to mediate both high (*i.e.* immune ligand) and low (*i.e.* tonic) level signaling and provide additional opportunities for pharmacological intervention beyond just ATP-competitive

All authors were or are employees of Merck & Co., Inc.
[1] Present address: University of Colorado, Boulder, CO.
[2] To whom correspondence should be addressed: 33 Avenue Louis Pasteur, Boston, MA 02115. Tel.: 617-992-3114; E-mail: james.miller2@merck.com.
[3] The abbreviations used are: SYK, spleen tyrosine kinase; ppITAM, dual-phosphorylated immune-receptor tyrosine-based activation motif; PTK, protein-tyrosine kinase; SH2, Src homology domain 2; GST, glutathione *S*-transferase; KD, kinase dead; up, unphosphorylated; CV, column volume.

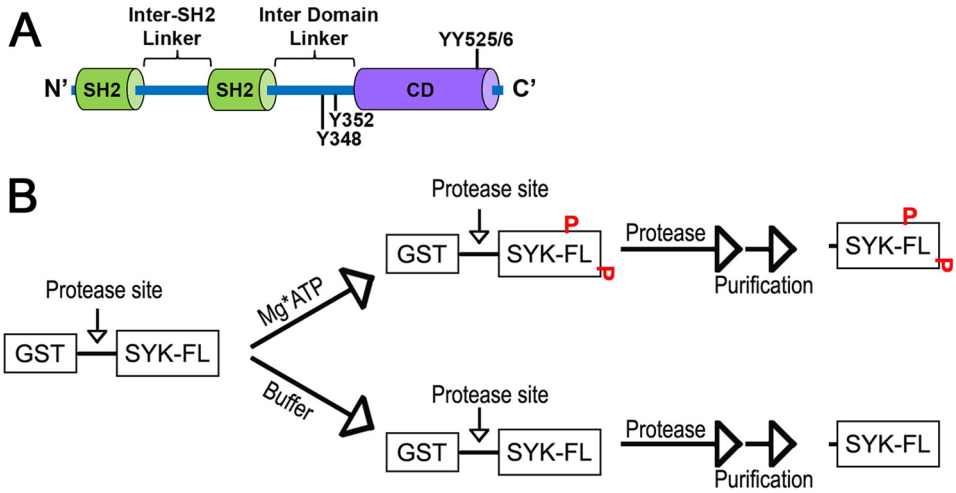

Figure 1. SYK domains and preparation of isoforms. *A,* domain architecture of SYK indicating the tandem SH2 domains and the catalytic domain (*CD*), with key regulatory phosphosites indicated. *B,* general scheme for preparation of untagged WT and mutant SYK proteins in the phosphorylated and unphosphorylated state.

kinase inhibitors. SYK activation could potentially be blocked by interrupting contact with ppITAM sequences, blocking auto- or transphosphorylation, or blocking the conformational transition from autoinhibited to the activated state. Accessing these alternative mechanisms requires a thorough understanding of the mechanism(s) driving SYK at each stage of its activation.

The molecular mechanism(s) by which SYK becomes activated/phosphorylated has been the subject of considerable study *in vitro* and in cells. One commonly cited activation mechanism is referred to as the "OR-gate." Based on *in vitro* studies with purified GSH *S*-transferase (GST)-tagged SYK proteins, Tsang *et al.* (18) propose that full and equivalent activation of SYK can occur through either binding to a phosphorylated ITAM containing peptide or by phosphorylation at residues Tyr-348 and/or Tyr-352 in the interdomain linker region (18). An alternative mechanism has also been proposed for both SYK (16) and ZAP70 (17). Rather than 2 equivalent paths to activation, binding to ppITAM sequences is proposed to induce a conformational change that relieves the autoinhibited conformation by disrupting the interaction of the tandem SH2 domain and the catalytic domain. This conformational change exposes key interdomain linker residues for phosphorylation by SRC family kinases and/or autophosphorylation, leading to full activation of SYK or ZAP70.

In vitro studies of SYK have been complicated by use of various constructs and preparations that are not directly comparable and/or contain fusion tags with secondary properties such as obligate dimerization. Cellular studies, whereas potentially more physiologically relevant, provide data that can be difficult to deconvolute into individual steps within the complex activation process. To address these questions, we utilized a novel approach to generate relevant and comparable SYK protein reagents. These preparations are generated from a single batch of recombinant cell lysate expressing a single GST-fused SYK construct. This lysate can be manipulated through downstream processing to generate directly comparable GST-tagged and tag-free SYK preparations in both the inactive (unphosphorylated) and active (phosphorylated) states. These preparations were utilized in continuous enzymatic assays of kinase activity, immunoblotting assays, and phosphoproteomic assays to test and refine mechanistic models. Our observations support a graduated activation mechanism involving a partially activated intermediate ppITAM-bound state that is primed for full activation by LYN.

Results and discussion

Characterization of recombinant SYK enzymes

We generated four isoforms of full-length human SYK (GST-pSYK, GST-upSYK, pSYK, and upSYK) using a single baculovirus expression construct to infect a single batch of *Sf*21 cells, followed by parallel purification procedures to ensure all purified proteins retain similar levels of well-folded enzyme. Among these, GST-upSYK and nontagged upSYK were prepared in a manner to maintain the lowest levels of phosphorylation, whereas GST-pSYK and nontagged pSYK were prepared to obtain the highest levels of total SYK phosphorylation achievable under *in vitro* conditions. The approach to prepare these reagents is outlined in Fig. 1*B*. Once purified, the differential levels of phosphorylation of both nontagged (pSYK *versus* upSYK) and GST-tagged (GST-pSYK *versus* GST-upSYK) SYK were confirmed by Western blot analysis (Fig. 2*A*). Specifically, a pan-antiphosphotyrosine antibody (Fig. 2*A*, *lanes 5–8*) was used to evaluate total phosphorylation of tyrosine residues and an anti-SYK antibody was used to ensure equal loading of the enzymes (Fig. 2*A*, *lanes 1–4*). Results showed little or no detectable phosphorylation of GST-upSYK (*lane 5*) and upSYK (*lane 7*), respectively, as compared with the high levels of phosphorylation of GST-pSYK (*lane 6*) and pSYK (*lane 8*). These results are consistent with MS data collected on a proteolytically-digested upSYK sample, which showed an estimated 5% total phosphorylation on tyrosine side chains of ionizable peptides (Table 1, column labeled *SYK*). The lower molecular weight bands seen in the GST fusions are likely minor proteolytic fragments of SYK that are removed during additional purification steps following tag cleavage.

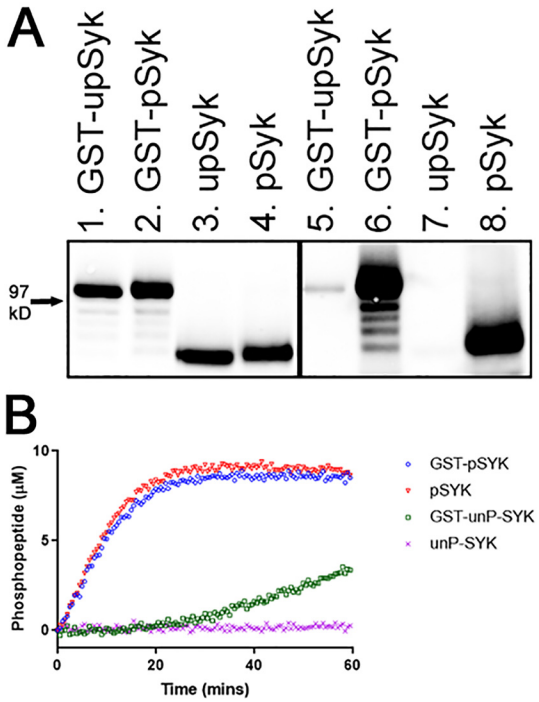

Figure 2. Properties of purified SYK isoforms. *A,* Western blotting illustrating the phosphorylation levels of the four SYK isoforms (*lanes 1* and *5,* 50 ng of GST-upSYK; *lanes 2* and *6,* 50 ng of GST-pSYK; *lanes 3* and *7,* 36 ng upSYK, and *lanes 4* and *8,* 36 ng of pSYK). *Lanes 1–4* were probed with mouse anti-human SYK to ensure equal loading of phosphorylated (designated as *p*) *versus* unphosphorylated (designated as up) SYK. The corresponding *lanes 5–8* were probed with a mouse anti-phosphotyrosine antibody to show phosphorylation levels for each of the four isoforms. The location of a molecular mass standard band migrating at 97 kDa is denoted with an *arrow*. *B,* phosphorylation of a generic peptide (Omnia® S/T peptide 7) by each SYK isoform was evaluated in a continuous kinetic Omnia kinase assay. Enzyme, ATP, and peptide concentrations used for all four kinase reactions were 4 nM, 35 μM, and 10 μM, respectively. The phosphorylated product was quantified relative to a standard curve. GST-pSYK (*blue circles*), pSYK (*red triangles*), GST-upSYK (*green squares*), and upSYK (*pink crosses*) are shown.

A previously developed (19) continuous kinetic assay was used to evaluate the ability of each SYK isoform to catalyze phosphorylation of a generic peptide substrate (Omnia® Y peptide 7, Invitrogen, referred to afterward as the Omina assay). Comparing equivalent concentrations of each SYK preparation in this assay, upSYK showed the lowest level of kinase activity, followed by GST-upSYK, whose activity was only slightly elevated. In contrast, a similar high level of substrate phosphorylation was observed with both GST-pSYK and pSYK (Fig. 2*B*). These results positively correlate with the phosphorylation levels of the purified enzymes, where pre-phosphorylation is likely responsible for inducing SYK to adopt an activated conformation. Based on our purification procedures, GST-pSYK and pSYK have similar levels of pre-phosphorylation, and as expected, no distinguishing differences in their activity profiles were observed. Under the conditions of our kinase reaction upSYK, which is most likely to exist in the autoinhibited conformation, is unable to spontaneously undergo the conformational change required for robust kinase activity. However, the GST-upSYK shows a slow increase in activity after a lag phase. Although GST-upSYK is also likely to be in the autoinhibited conformation initially, the known dimerization of GST (20), likely brings two SYK molecules into close proximity, enhancing activation via transphosphorylation.

GST-upSYK protein achieves robust kinase activity through pre-phosphorylation or phosphorylated ITAM binding

Several cell-free studies have investigated SYK activation via autophosphorylation, SRC family kinase-mediated phosphorylation, and phosphorylated ITAM (ppITAM) mediated activation (18, 19, 21–23). Tsang *et al.* (18) were the first to publish results using full-length recombinant SYK protein, and their OR-gate model for activation has been widely cited. In brief, their study suggests full-length SYK protein is equivalently activated by either pre-phosphorylation or by binding to ppITAM sequences. However, the inability of ppITAM to activate SYK in B cell lysates (18) and the activating effects of a GST-SYK fusion noted above (Fig. 2*B*), led us to further interrogate the OR-gate mechanism. Using our directly comparable GST-tagged and tag-cleaved upSYK constructs in the Omnia kinase assay, we first examined the influence of an FcεRI ppITAM peptide (referred to as ppITAM throughout) on SYK activation.

Consistent with the results of Tsang *et al.* (18), GST-upSYK alone (Fig. 3*A*, *open circle*) showed an initial lag phase over the course of 15 to 20 min, followed by a slightly elevated steady-state rate. In the presence of 1 μM ppITAM (*open circles*), GST-upSYK exhibited an instant steady-state rate comparable (~70%) to pre-phosphorylated GST-pSYK (not shown). Although slightly slower than the GST-pSYK enzyme, the addition of ppITAM to GST-upSYK enabled this enzyme to turn over at a rate equivalent to that observed with addition of LYN alone (*open squares*) or LYN and ppITAM (*open triangles*). It should be noted that GST-pSYK was produced by incubation with high ATP (1 mM) at ambient temperature for 25 min followed by an extended overnight incubation at 4 °C (see "Experimental procedures"). It is therefore not surprising that this enzyme would have slightly higher kinase activity than that observed in the GST-upSYK/ppITAM and LYN reactions, where the ATP concentration was kept near K_m values (35 μM for GST-pSYK and pSYK and 10 μM for GST-upSYK and upSYK). Phosphorylation of specific SYK residues over time was also monitored using Western blots, and the accumulation of Tyr-352 and Tyr-525/Tyr-526 phosphorylation signals were comparable with those shown by Tsang *et al.* (18) (data not shown). Together, these results suggest that ppITAM is capable of rapidly activating GST-upSYK to the same extent as GST-pSYK, consistent with the OR-gate hypothesis for SYK activation.

ppITAM binding to monomeric upSYK fails to fully activate SYK

We next examined the influence of ppITAM on activation of upSYK lacking the GST fusion tag. Increasing concentrations of a ppITAM peptide derived from the FcεRI adapter were added to either pSYK or upSYK and enzymatic rates were measured using the Omnia assay (Fig. 3*B*). The ppITAM had no effect on the level of pSYK activity. However, addition to untagged upSYK resulted in a ~7-fold increase over the low basal activity of upSYK with an EC_{50} of 124 ± 2 nM. Despite the ppITAM-dependent increase in kinase activity, the rate at saturation was only ~15% of the prephosphorylated SYK.

Table 1
SYK phosphospecific analysis using mass spectrometry
Reactions to assess the sites of SYK autophosphorylation were conducted in the presence or absence of ppITAM and/or LYN and quenched at the indicated reaction time points. Each reaction was then subjected to proteolysis. Phosphoproteomic analysis of the resulting ionizable peptides was performed to assess the fractional phosphorylation at the indicated serine, threonine, or tyrosine residues.

Phosphorylation sites	SYK	SYK + ATP	SYK + ATP + ppITAM	SYK + ATP + LYN	SYK + ATP + ppITAM + LYN	SYK + ATP + ppITAM + LYN	SYK + ATP + ppITAM + LYN
Reaction time	Up[a]	5 min	5 min	5 min	15 s	30 s	5 min
pTyr-364	1	1	1	2	1	2	5
pTyr-203	2	2	2	2	2	2	2
pTyr-630 (629)	2	3	2	2	2	2	2
pTyr-631	<1	<1	<1	<1	<1	<1	<1
pTyr-131	ND[b]	ND	<1	17	ND	<1	5
pTyr-323	<1	<1	37	40	7	16	70
pTyr-296	ND	30	7	43	ND	2	68
pTyr-352	ND	<1	2	10	18	25	22
pTyr-348 + pTyr-352	ND	<1	3	32	4	10	43
pTyr-345 + pTyr-348 + pTyr-352	ND	ND	<1	<1	<1	<1	<1
pTyr-526	ND	ND	ND	25	2	5	21
pTyr-525 + pTyr-526	ND	ND	ND	7	ND	<1	3

[a] The notation "up" denotes unphosphorylated.
[b] ND indicates not determined.

To assess the effect of ppITAM on upSYK autophosphorylation we performed timed reactions of upSYK and MgATP with or without ppITAM. Western blots of the quenched reactions were probed with antibodies specific for phosphosites within the interdomain region (Tyr-323, Tyr-348, Tyr-352) and the activation loop (Tyr-525/Tyr-526) (Fig. 3*C*, *lanes 1–6*). Samples from these kinase reactions were also examined using quantitative phosphoproteomic MS (Table 1, columns labeled SYK + ATP and SYK + ATP + ppITAM). Incubation of upSYK with ATP showed no significant phosphorylation of any residue other than Tyr-296 (Table 1, column labeled SYK + ATP), which is not thought to be involved in SYK activation (24). Consistent with the modest increase in kinase activity with ppITAM (Fig. 3*B*), minimal phosphorylation was observed for interdomain or activation loop tyrosines except for Tyr-323. The ppITAM peptide is not sufficient to fully activate monomeric SYK under these conditions, in contrast to the results observed with GST-tagged upSYK.

Full activation of SYK requires ppITAM engagement and phosphorylation mediated by LYN

The recruitment of SYK to ppITAM sequences in immune receptor-associated proteins is tightly coupled to other events, such as the recruitment of specific SRC family kinases such as LYN (25). The contributions of these separate factors to SYK activation are difficult to assess in a cellular context. However, the Omnia assay offers a means to study the separate and combined effects of ppITAM and LYN on upSYK activation. Omnia kinase assays were conducted under the following conditions: 1) upSYK alone; 2) upSYK + ppITAM; 3) upSYK + LYN; and 4) upSYK + ppITAM + LYN. All reactions were run in parallel and real-time kinetic data were collected over the course of 60 min (Fig. 3*D*). LYN and ppITAM in combination have the greatest effect on upSYK activity and are comparable (~70%) to that of pre-phosphorylated SYK and pre-phosphorylated GST-SYK (Fig. 2*B*, *open circles* and *squares*). These data demonstrate that the lower activity seen with either ppITAM or LYN alone is not due to misfolded or inactive unphosphorylated kinase and indicates that upSYK exists in an autoinhibitory conformation that can be fully activated under appropriate conditions.

These results suggest that ppITAM and LYN operate in tandem rather than independently. A key tenet of an OR-gate mechanism is that both stimuli are equivalent and not additive (26). The nonequivalence and additivity of ppITAM and LYN show that a more nuanced model is required to describe SYK activation. Other data reported by Tsang *et al.* (18) may be reinterpreted to support a more complex model of activation than the OR-gate. When Ramos B cell lysates were examined for SYK activity with and without the addition of ppITAM, little difference in activity was observed. However, when SYK was immunoprecipitated from these lysates, robust activation by a ppITAM peptide was observed. The immunoprecipitation step may serve to bring SYK molecules into forced proximity, comparable with the obligate dimerization of GST fusions. Similar proximity-based activation of SYK was reported by Antenucci *et al.* (27) who observed that monomeric β3-integrin peptides (which bind to SYK at a site independent of ppITAM) have no effect on upSYK activity. However, clustering of β3-integrins prior to addition of SYK promotes robust SYK activation.

LYN-mediated phosphorylation of SYK-Tyr-352 is accelerated by ppITAM engagement

Temporal analysis of SYK phosphorylation in activated Ramos B cells demonstrates residues in the interdomain linker and activation loop are phosphorylated within minutes of cellular activation (28). Our biochemical data indicate that phosphorylation by LYN and binding to ppITAM make distinct but additive contributions to SYK activation. To better understand the molecular mechanism(s) behind these observations, phosphorylation of SYK on Tyr-323, Tyr-348, Tyr-352, and Tyr-525/Tyr-526 was assessed by Western blotting and phosphoproteomic MS.

The immunoblotting data of upSYK incubated with LYN shows a considerably faster and more extensive phosphorylation than was observed with upSYK alone or upSYK with ppITAM (compare Fig. 3*C*, *lanes 1–6 versus lanes 11–14*). Tyrosine 323 is the most heavily phosphorylated residue but Tyr-348, Tyr-352, and Tyr-525/Tyr-526 all show increasing phosphorylation over time. Most striking, however, is the combination of LYN and ppITAM (Fig. 3*C*, *lanes 7–10*) where there

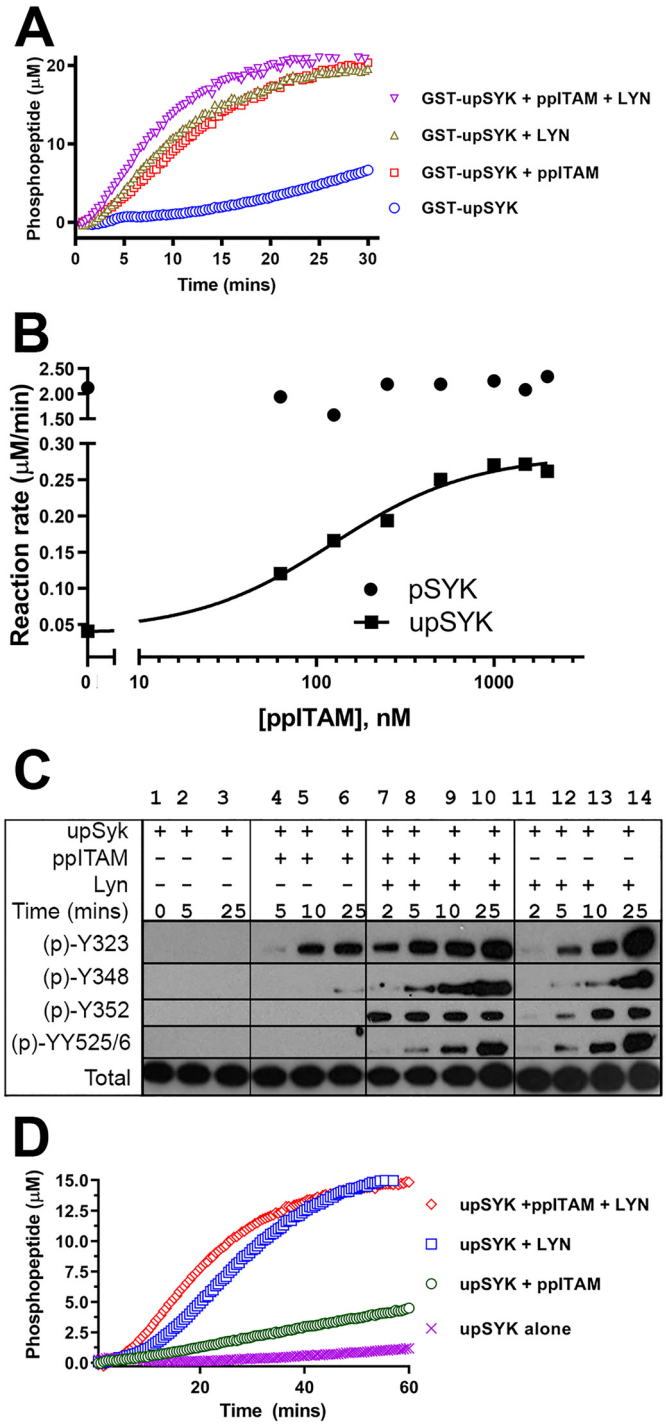

Figure 3. ppITAM- and LYN-mediated activation of SYK isoforms. *A,* kinetic profiles of Omnia kinase reactions of GST-upSYK alone (*blue circles*), GST-upSYK + ppITAM (*red squares*), GST-upSYK + LYN (*green triangles*), and GST-upSYK + ppITAM + LYN (*pink inverse triangles*) are shown. Enzyme (4 nM), ATP (35 μM), and peptide (10 μM) concentrations were kept constant in all four reactions. *B,* effect of increasing concentrations of ppITAM on the rate of upSYK or pSYK phosphorylation of Omnia S/T peptide 7. Reagent concentrations were 25 nM of each SYK protein, 35 μM ATP, and 10 μM Omnia peptide. The *solid line* represents a fit to the 4-parameter logistic equation using the no ppITAM rate to define the minimum. The maximum, Hill slope, and EC_{50} values were floated to obtain the best nonlinear least squares fit to the equation. *C,* Western blots (region migrating at 65–80 kDa) showing a time course of site-specific SYK tyrosine phosphorylation in the presence or absence of ppITAM and/or LYN. Reaction conditions are described under "Experimental procedures." *Lane 1* corresponds to a negative control reaction, which was immediately quenched. Phosphorylation signals were also shown for upSYK alone (*lanes 2* and *3*), upSYK + ppITAM (*lanes 4–6*), upSYK + ppITAM + LYN (*lanes 7–10*), and upSYK + LYN (*lane 11-14*). *D,* kinetic data were acquired identically to that in *A* except GST-upSYK was replaced with upSYK, and their respective kinetic profiles are as follows: upSYK alone (*pink crosses*), upSYK + ppITAM (*green circles*), upSYK + LYN (*blue squares*), and GST-upSYK + ppITAM + LYN (*red diamonds*) are shown. Enzyme (4 nM), ATP (35 μM), and peptide (10 μM) concentrations were kept constant in all four reactions.

is rapid phosphorylation of Tyr-323 and saturation of Tyr-352 phosphorylation within 2 min. Tyrosine 348 and Tyr-525/Tyr-526 also show enhanced phosphorylation, which increases across the time course.

The phosphorylation results acquired using immunoblotting were compared with more quantitative MS data. To better resolve the kinetics of phosphorylation, samples were collected within the first few minutes of the incubation. Addition of LYN to upSYK shows greater phosphorylation of Tyr-352 and slightly slower phosphorylation of Tyr-348 and Tyr-525/Tyr-526 (Table 1, columns with combinations including LYN). However, in the presence of LYN and ppITAM, phosphorylation of Tyr-352 is even more rapid, reaching near saturation in ~15 s, suggesting that this is the primary site of LYN phosphorylation and is facilitated by ppITAM binding, consistent with earlier reports (7). Phosphorylation of Tyr-348 and Tyr-525/Tyr-526 occur at a similar rate that is slower than phosphorylation of Tyr-352. It is not clear if phosphorylation of Tyr-352 is a prerequisite for phosphorylation of Tyr-348; however, peptides containing pTyr-348 were not detected in the absence of pTyr-352. Consistent with this observation, a previous study of stimulated B cells showed that SYK phosphorylation peaks at 2 min for the interdomain residues Tyr-348 and Tyr-352 with only monophosphorylated Tyr-352 and doubly phosphorylated Tyr-348 + Tyr-352 peptides reported (28). Although Tyr-296 is rapidly phosphorylated under all conditions of our study, it does not correlate with kinase activity.

ppITAM accelerates LYN-mediated interdomain phosphorylation in the presence of kinase dead (KD)-SYK

The increase in SYK activity in the presence of ppITAM and LYN appears to best correlate with the accelerated rate of Tyr-352 phosphorylation, suggesting that ppITAM binding may facilitate LYN phosphorylation of this site. To address the potential contribution of autophosphorylation and to understand if LYN is capable of phosphorylating Tyr-323 and Tyr-525/Tyr-526, we generated a K402R "kinase dead" mutant SYK (SYK-KD), which is <4% as active as WT SYK in the Omnia assay (data not shown). Phosphorylation of upSYK-K402R by LYN was evaluated in the presence and absence of ppITAM (Fig. 4). No phosphorylation was detected at any of the four tested sites with upSYK-K402R alone or upSYK-K402R + ppITAM within 25 min. However, all four residues of upSYK-K402R are phosphorylated by LYN with Tyr-352 and Tyr-348 phosphorylation significantly enhanced in the presence of ppITAM. These results suggest binding of ppITAM makes the interdomain region more susceptible to phosphorylation. In line with this observation, the structure of full-length upSYK shows Tyr-352 is more exposed to solvent (and presumably more accessible to phosphorylation) than Tyr-348, which participates in a hydrogen bond with Ala-142 in the interdomain linker (16).

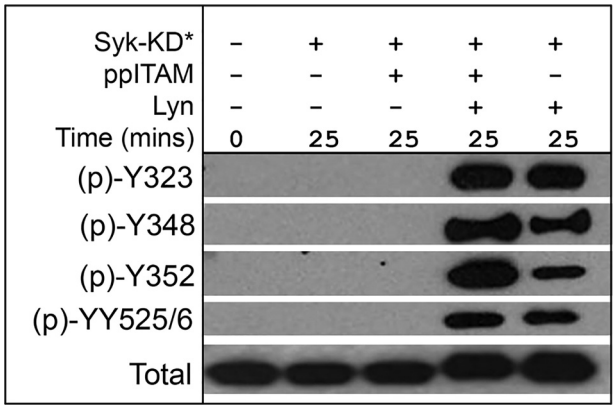

Figure 4. ppITAM binding accelerates LYN-mediated phosphorylation of kinase dead-SYK (*SYK-KD*). SYK-KD was treated with LYN, ATP, and with or without ppITAM for the indicated times. Reactions were subjected to Western blotting with phosphosite-specific antibodies as described under "Experimental procedures." The region migrating at 65–80 kDa is shown.

Phosphorylation site mutants confirm interdomain phosphorylation is critical for SYK activation

To study the role of specific phosphosites on SYK kinase activity we generated a panel of recombinant full-length upSYK and pSYK proteins with specific phosphorylation sites mutated from tyrosine to phenylalanine. In contrast to earlier studies of phosphosite mutations, we utilized the approach described in Fig. 1*B* to purify directly comparable unphosphorylated and phosphorylated SYK proteins without a GST fusion tag.

The intrinsic kinase activity of each upSYK mutant was assessed in the Omnia assay and reaction time courses are shown in Fig. 5*A*. As previously observed (Fig. 2*B*) WT upSYK shows minimal activity as does the Y348F mutant. However, other mutants showed activity appreciably above background. Most notable are the interdomain mutants Y352F and Y323F and the activation loop mutants Y525F/Y526F, which showed nonlinear increases in activity suggesting slow autoactivation of these proteins. The Y131F and Y296F mutants also showed modest autoactivation, which was unexpected given that these residues are not expected to play a role in maintaining the autoinhibited conformation.

We next tested the kinase activity of the prephosphorylated mutant SYK proteins (Fig. 5*B*). All proteins showed an initial linear reaction rate suggesting no further autoactivation occurred during the assay. The WT protein, the Y296F and Y131F mutants as well as two of the interdomain mutants (Y323F and Y352F) all show robust kinase activity. However, the activation loop mutants Y525F/Y526F and the interdomain mutant Y348F were clearly impaired in their kinase activity. Even with additional preincubation with 1 mM ATP, ppITAM and LYN, these two mutants could not be further activated.

We next studied the phosphorylation state of key residues in the unphosphorylated and prephosphorylated mutant proteins by Western blotting. WT kinase served as a reference for standard phosphorylation levels at each site. Equimolar quantities of each SYK enzyme were loaded onto SDS-PAGE and probed with phosphospecific antibodies. As expected, no phosphorylation was detected for all untreated samples (lanes denoted with *u* in the phosphorylation status line of Fig. 5*C*). With the prephosphorylated samples, none of the specifically mutated residues showed detectable phosphorylation. The Y131F, Y296F, and Tyr-323 mutants showed phosphorylation at all tested WT residues, although Y296F had reduced total phosphorylation. Interdomain mutant Y352F exhibits strong phosphorylation of Tyr-323, Tyr-348, and Tyr-525/Tyr-526 consistent with its robust kinase activity (Fig. 5*B*). The interdomain mutant Y348F shows an intriguing pattern. Robust phosphorylation of Tyr-323 is seen, indicating the protein is not misfolded. However, there is no detectable phosphorylation of either Y352F or the activation loop tyrosines 525/526. The severely impaired kinase activity of this mutant suggests a critical role for Tyr-348 in the transition from the autoinhibited to the activated state. This result was unexpected, however, given the previously mentioned hydrogen bond between Tyr-348 and Ala-142 (16). The mutation of Tyr-348 to phenylalanine would be expected to preclude formation of this hydrogen bond and therefore could destabilize the inactive conformation. However, other interactions must be more important in maintaining the integrity of the autoinhibited conformation. The activation loop mutants Y525F/Y526F also show an unexpected pattern. Modest phosphorylation is observed at Tyr-323 and Tyr-352, but none is detected at Tyr-348. The low kinase activity of this mutant may be due to the lack of activation loop and/or Tyr-348 phosphorylation highlighting the link between ppITAM binding and the accessibility of Tyr-348 for phosphorylation.

Interdomain and activation loop phosphorylation site mutants exhibit differences in activation with ppITAM and LYN

The previous experiment exploring the role of specific phosphorylation sites in SYK autoactivation suggests distinct roles for Tyr-348 and Tyr-352 and the activation loop Tyr-525/Tyr-526. To assess if these residues are also involved in activation when ppITAM and/or LYN are present, we again utilized the Omnia assay. The upSYK-Y352F and prephosphorylated SYK-Y352F proteins were tested with and without LYN, ppITAM, or both. Reaction progress curves are shown in Fig. 6, *A* and *B*, for the unphosphorylated and phosphorylated proteins, respectively. The upSYK-Y352F mutant shows a reduced response to ppITAM relative to WT upSYK (Fig. 3*D*) and no additional activation from the combination of ppITAM + LYN relative to that afforded by LYN alone. Like WT SYK, the prephosphorylated Y352F-SYK shows robust activity with no additional activation seen upon addition of ppITAM, LYN, or both. A very different profile is observed with the SYK-Y348F proteins. The unphosphorylated and the prephosphorylated Y348F proteins are similar in that addition of ppITAM or LYN results in partial activation and the combination provides maximal activation. This result with the prephosphorylated Y348F fusion protein is surprising and indicates that the prephosphorylation reaction conducted prior to GST cleavage (Fig. 1) was unsuccessful at fully activating the Y348F mutant. This may reflect that the autoinhibited conformation of Y348F is quite stable and therefore resistant to autoactivation, even in the context of an obligate dimer. Phosphorylation of Tyr-352 may serve as a prerequisite to access Tyr-348, whose phosphorylation then acts as the principal driver for full SYK activation. The unphosphorylated and prephosphorylated activation loop mutant (Y525F/Y526F) behaved nearly identically to Y384F (data not shown)

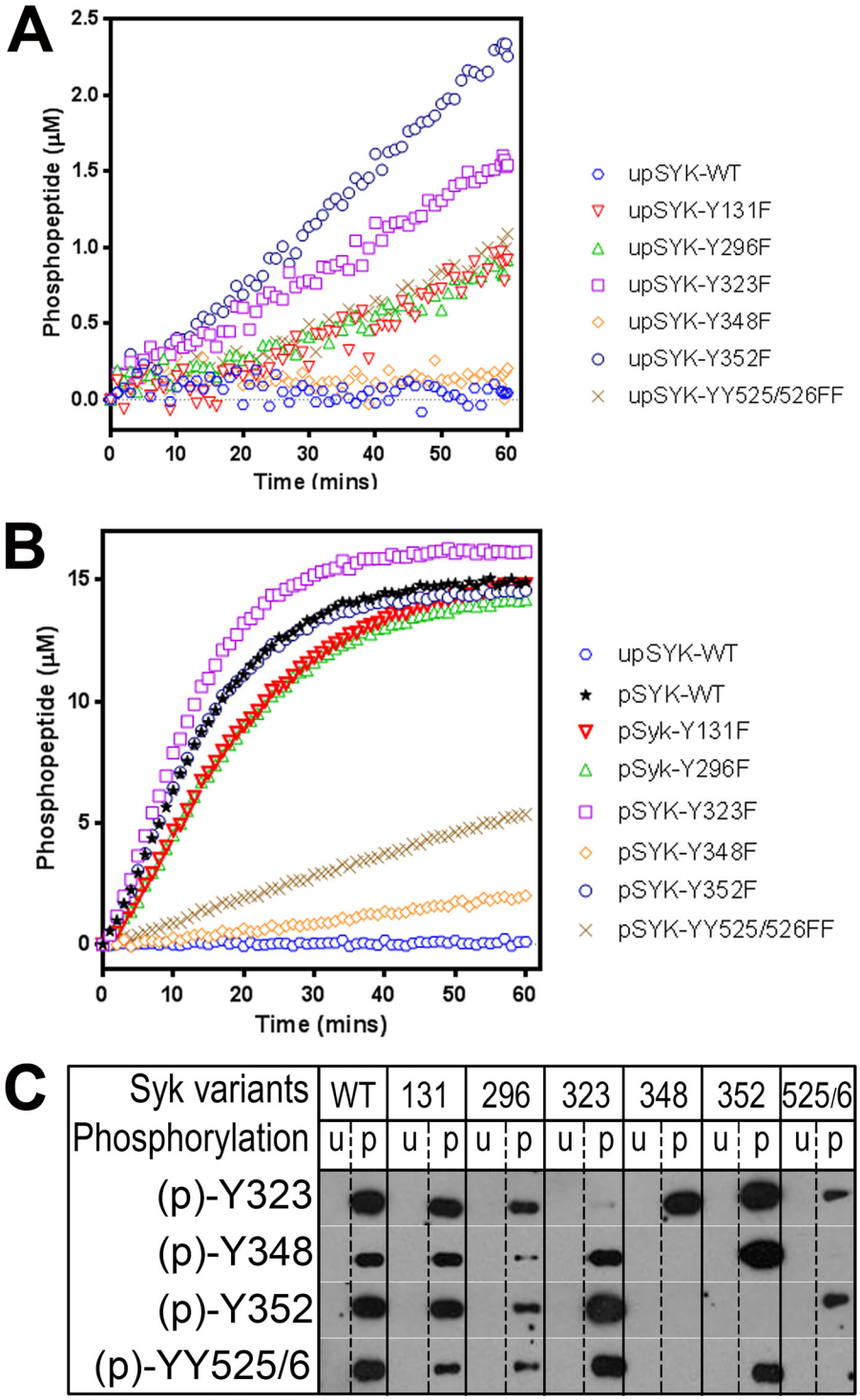

Figure 5. Effects of site-directed mutations on SYK kinase activity. *A,* the basal kinase activity of each unphosphorylated mutant SYK was evaluated relative to the WT protein using the Omnia kinase assay. Enzyme (4 nM), ATP (35 μM), and peptide (10 μM) concentrations were kept constant in all reactions. *B,* the basal kinase activity of each phosphorylated mutant SYK was evaluated relative to the WT protein. Reaction conditions are identical to those of *A*. *C,* Western blots (region migrating at 65–80 kDa) examining site-specific SYK tyrosine phosphorylation of unphosphorylated and prephosphorylated WT and mutant SYK proteins. Conditions are described under "Experimental procedures."

and was resistant to autoactivation. The site-specific mutant data and the similar timing of phosphorylation (Fig. 3*C* and Table 1) suggest there is interplay between phosphorylation of Tyr-348 and Tyr-525/Tyr-526 in the activation loop. The inability to phosphorylate Tyr-348 and/or the activation loop may favor return to the autoinhibited conformation.

A revised model for SYK activation

Collectively our data suggest a complex mechanism of SYK activation that is more consistent with the nuanced physiological roles of SYK than would be possible under the constraints of a literal OR-gate mechanism. Recent structural and biochemical studies of the closely related kinase ZAP70 and full-

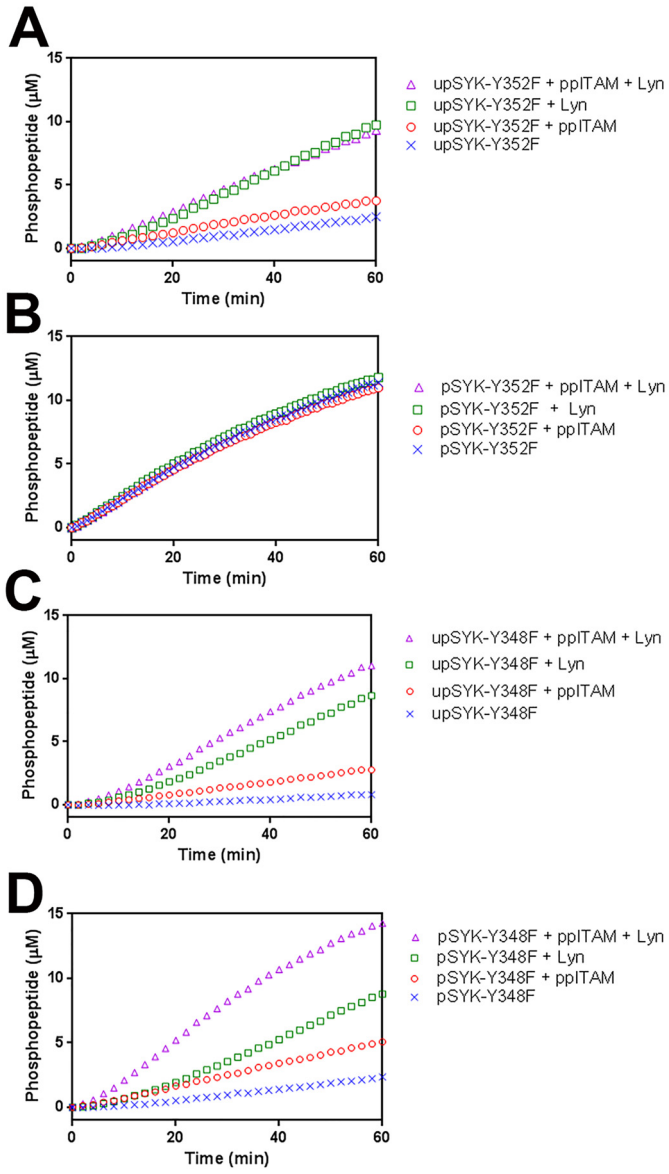

Figure 6. Effects of ppITAM and LYN on the kinase activity of SYK phosphosite mutants. Kinetic profiles of Omnia kinase reactions of: *A,* upSYK-Y352F; *B,* pSYK-Y352F; *C,* upSYK-Y348F; *D,* pSYK-Y348F. Each *panel* shows the kinetic profiles of Omnia kinase reactions of up/pSYK alone (*blue crosses*), up/pSYK + ppITAM (*red circles*), up/pSYK + LYN (*green squares*), and up/pSYK + ppITAM + LYN (*pink triangles*). Enzyme (4 nM), ATP (35 μM), and peptide (10 μM) concentrations were kept constant in all reactions.

length SYK provide a mechanistic framework that is consistent with and can be augmented by our data (16, 17). In this mechanism, ppITAM binding is proposed to induce a conformational change in ZAP70/SYK that results in release of the tandem SH2 domains from the kinase domain, exposing residues within the interdomain region to phosphorylation by LCK (ZAP70) or LYN (SYK). This is hypothesized to subsequently alter the mobility of the activation loop enabling its phosphorylation and thereby full activation of SYK/ZAP70. A refinement of this model, informed by our data, is proposed in Fig. 7. Binding of ppITAM makes Tyr-352 accessible to phosphorylation by LYN, which facilitates subsequent phosphorylation of Tyr-348 and the activation loop. Our kinetic data and observation that phosphorylation of Tyr-352 and Tyr-348 are not equivalent and that activation loop phosphorylation and Tyr-348 phosphorylation are tightly linked support the hypothesis that ppITAM-bound SYK represents an intermediate activation state. This could allow graduated levels of SYK kinase activity, depending on the state of interdomain and activation loop phosphorylation. Graduated activity of SYK may be important for a cellular phenomena such as tonic signaling where complete activation may not be desirable. Additional studies are required to establish if a graduated activation mechanism is observed within cells.

Experimental procedures

Cloning and expression of all SYK isoforms

The full-length SYK gene from NCBI reference NP_003168.2 was synthesized with an N-terminal sequence coding for the PreScission protease site (pp: LEVLFQGP) and subcloned into a pFastBac1 vector (Invitrogen) that was modified with an in-frame N-terminal GST tag (GenScript). This resulting construct, when translated, yields a GST-(pp)-SYK (pp will be omitted from here onward) protein, where monomeric SYK may be generated by cleavage with PreScission protease (GE Healthcare). Procedures used to generate SYK baculovirus to overexpress this fusion protein are described in more detail here. First, the pFastBac1 GST-pp-SYK vector was transformed into MAX Efficiency® DH10Bac™ competent cells, which were amplified in LB medium and from which recombinant bacmid DNA was isolated according to the Invitrogen Bac-to-Bac Baculovirus Expression Systems manual. The isolated recombinant bacmid DNA was then transfected into *Spodoptera frugiperda Sf*21 cells to generate and isolate SYK-P1 virus 72 h post-transfection. P2 virus was generated by infecting a suspension of *Sf*21 cells with P1 virus with a dilution of 1:150 for 72 h. Using P2 virus, large scale (1–5 liters) infections were performed (virus dilution of 1:4000) to overexpress sufficient amounts of SYK.

Purification of all SYK isoforms

Four liters of infected *Sf*21 cells were resuspended in 200 ml of lysis buffer (50 mM Tris, pH 8, 300 mM NaCl, 10% glycerol, 0.5 mM EDTA, 2 mM DTT, 0.05% Triton X-100, and a Roche protease inhibitor mixture tablet). The resuspended cells were lysed in two freeze-thaw cycles using liquid nitrogen, followed by high-speed centrifugation at 40,000 rpm for 2 h (Beckman Coulter; Type 45 Ti fixed-angle rotor, part number 339160) to remove cell debris from soluble proteins. The cleared supernatant was directly added to 5 ml of pre-equilibrated (equilibration buffer: 500 mM NaCl, 5% glycerol, 50 mM Tris, pH 8, 0.025 mM EDTA, and 1 mM DTT) GSH beads (GE Healthcare) and protein was bound in batch mode for 30 min on ice. The bead suspension was then poured into a free-standing gravity column and washed with 40 column volumes (CV) of equilibration buffer or until no protein was detected from the wash (wash buffer: 1 M NaCl, 5% glycerol, 50 mM Tris, pH 8, 0.025 mM EDTA, and 1 mM DTT). At this point, 1 CV of low salt buffer (buffer A: 25 mM HEPES, pH 6.8, 5% glycerol, and 2 mM DTT) was passed through the beads prior to elution of the target protein. GST-upSYK (up = un-phosphorylated) was eluted

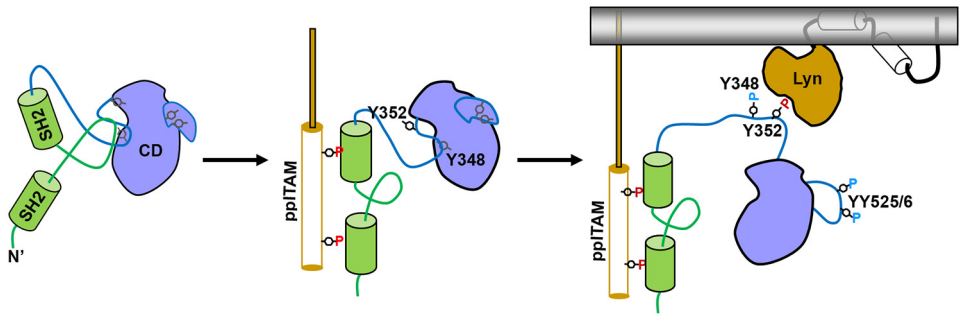

Figure 7. Proposed model of SYK activation by phosphorylated ITAM sequences, interdomain phosphorylation, and activation loop phosphorylation.

from the affinity column with ~50 ml of elution buffer (25 mM HEPES, pH 6.8, 5% glycerol, 2 mM DTT, and 10 mM reduced GSH; buffer was adjusted to pH 6.8 after the addition of reduced GSH). The eluted GST-upSYK enzyme has no detectable tyrosine phosphorylation and starting with this isoform, three additional isoforms (GST-pSYK, untagged upSYK, and pSYK) of SYK were generated. To do this, half of the total protein was phosphorylated by adding 10 mM $MgCl_2$ and 1 mM ATP for 25 min at room temperature. The two halves (phosphorylated and unphosphorylated) of GST-SYK were again divided into equal volumes, where half of the phosphorylated and half of the unphosphorylated proteins were treated with PreScission protease overnight at 4 °C to cleave the GST tag from SYK. It should be noted that ATP/$MgCl_2$ were not removed prior to adding PreScission protease, thus SYK could acquire additional phosphorylation during the overnight incubation at 4 °C. The final four isoforms of SYK were: GST-upSYK, GST-pSYK, upSYK, and pSYK, and all were further purified on an anion exchange column. A 1-ml Q-Sepharose column (GE, catalog number 17-1153-01) was pre-equilibrated with 10 CV of buffer A. Each of the four forms of SYK was loaded and washed to remove unbound proteins. Under these buffer conditions, GST was immediately eluted from this column upon loading in both the flow-through and washed fractions. A 0 to 1 M NaCl gradient (buffer B: 1 M NaCl, 25 mM HEPES, pH 6.8, 5% glycerol, and 2 mM DTT) was applied to partition SYK from the remaining bound impurities. Fractions were selected from UV-active peaks in the gradient chromatogram and resolved on a 4–12% SDS gel. From the Coomassie-stained gel, fractions containing homogenous SYK were pooled and buffer exchanged into the final storage buffer (150 mM NaCl, 5% glycerol, 25 mM Tris, pH 7.5, and 2 mM DTT) using a Millipore filtration device (Millipore; 10,000 MWCO). SYK was concentrated and stored at −80 °C. It should be noted that all four isoforms of SYK were treated identically or similarly in terms of temperature of the sample and the duration of the purification, regardless if pre-phosphorylation or PreScission protease cleavage were performed. The levels of phosphorylation for all four isoforms were evaluated on Western blots, probed with total SYK (BD Biosciences mouse anti-human SYK, catalog number 51-9002493) and phosphotyrosine antibodies (Millipore mouse antiphosphotyrosine, clone 4G10®, catalog number 05-321) (Fig. 1).

Omnia assay

SYK enzymatic activity was monitored using the Omnia® Kinase Assay system from Invitrogen. Peptide substrate (Y-peptide 7, Invitrogen catalog number KNZ3071) contains the unnatural amino acid SOX. Upon phosphorylation of the peptide, Mg^{2+} is chelated to form a bridge between the Sox moiety and the phosphotyrosine resulting in increase in fluorescence (29). Reaction progress is monitored with a SpectraMax 2 plate reader (Molecular Devices) in kinetic mode using an excitation wavelength at 360 nM and an emission wavelength at 455 nM. Data points are collected every 10–30 s. The assay is performed in 15 mM Tris buffer, pH 7.5, supplemented with 20 mM $MgCl_2$, 0.01% Tween 20, and 2 mM DTT. The reaction volume was 20 μl in a 384-well black low volume nonbinding surface plate (Corning catalog number 3820). The concentrations of reaction components (*e.g.* SYK, LYN, ppITAM, and ATP) are specified in the figure captions.

Kinase assay and Western blot analysis

Conditions for kinase assays performed for Western blot analysis were 40 nM SYK and LYN, 250 nM ppITAM peptide (GenScript; Ac-GV(pY)TGLSTRNQET(pY)ETLKHE-NH_2, Ac = acetylation and NH_2 = amidation), and 30 μM ATP. Each reaction was initiated with ATP at ambient temperature and for the negative control, ATP was replaced with 1× kinase buffer (10 mM HEPES, pH 7.5, 2 mM $MgCl_2$, 0.002% Brij-35, 0.2 mM EGTA, 0.05% BSA, and 2 mM DTT). At specific time points following the addition of ATP, an aliquot of the reaction was quenched by adding 4× SDS-PAGE loading buffer (Invitrogen) supplemented with 20 mM EDTA. For WT (wt) and all SYK variants except upSYK-Y348F, 20 μl of the quenched reaction was boiled for 5 min and loaded onto a precast 4–12% SDS-PAGE (Invitrogen). The gel was electrophoresed for 90 min with constant voltage of 150 or until loading dyes migrated off the bottom. In the case of SYK-Y348F, 75 μl of the original quenched reactions were boiled for ~30 min to reduce the volume to ~25 μl prior to loading onto gel. Resolved protein bands were transferred onto nitrocellulose membrane using an iBOT machine (Independence Technology L.L.C.). Each kinase reaction was probed with five SYK phosphospecific antibodies (Cell Signaling Technology (1:500 dilution): SYK-Y323, catalog number 2715S; SYK-Y352, catalog number 2701; SYK-YY525/526, catalog number 2711S; BD Biosciences (1:200 dilution): SYK-Y348, catalog number 558167) to quantitate the levels of

phosphorylation at specific time points during the kinase reaction. For each set of experiments, a blot was randomly selected to be stripped and reprobed with a total SYK antibody (BD Biosciences: 1:1000 dilution, catalog number 51-9002493) to ensure accurate loading of the samples at all time points for each kinase reaction. For blots that were analyzed using chemiluminescence technology, anti-mouse and anti-rabbit secondary antibodies were used at 1:10,000 dilutions in 5% milk. For blots analyzed with LI-COR (LI-COR Biosciences) technology, goat anti-mouse (Odyssey IRDye 800 CW, catalog number 926-32210) and goat anti-rabbit (Invitrogen Alexa Fluor 680, catalog number A21076) were also used at 1:10,000 dilutions in Odyssey blocking buffer (LI-COR, catalog number 927-40000). These blots were scanned and analyzed using Odyssey software.

Mass spectrometry analysis

Phosphopeptide stoichiometry estimations using recombinant full-length untagged SYK was subjected to SDS-PAGE. The gel slices containing SYK from all treatment conditions were exercised, reduced, and alkylated prior to enzymatic digestion using LysC, trypsin, and AspN for maximum sequence coverage. The resulting peptides were analyzed individually by a reverse-phase nano-LC system (1200 series HPLC system; Agilent Technologies, Palo Alto, CA) online-coupled with a LTQ Orbitrap hybrid mass spectrometer (Thermo Electron, Bremen, Germany) as described (30). Acquired MS/MS data were searched against the SYK database obtained from National Center for Biotechnology Information (NCBI) with SEQUEST (31). Each MS/MS spectra exhibiting possible phosphorylation was manually validated. Areas under the ion chromatographic curves were manually determined using the "add peaks" tool in Qual Browser version 2.0 program (Thermo Electron). Percentage of phosphorylation per phosphopeptide was calculated by dividing the ion current of the specific peptide of interest by the sum of the ion current for the peptide in all observed charge states and modified forms (32). Due to the potential differences in ionization efficiencies among phosphorylated and nonphosphorylated peptides at various modified forms, the reported percentage of phosphorylation for each peptide may not represent physiological percentages for each modified site, and serves as a basis of comparison among samples from various *in vitro* kinase conditions.

Author contributions—M. S. M., L. R., A. C., B.-S. P., and J. R. M. conceptualization; M. S. M., L. R., A. C., B.-S. P., and J. R. M. formal analysis; M. S. M., L. R., A. C., B.-S. P., and J. R. M. supervision; M. S. M., A. R., L. R., and B.-S. P. validation; M. S. M., A. R., L. R., A. C., B.-S. P., and J. R. M. investigation; M. S. M., A. R., L. R., A. C., B.-S. P., and J. R. M. visualization; M. S. M., A. R., L. R., A. C., B.-S. P., and J. R. M. methodology; M. S. M., L. R., A. C., B.-S. P., and J. R. M. writing-original draft; M. S. M., A. R., L. R., A. C., B.-S. P., and J. R. M. writing-review and editing; A. R., L. R., and B.-S. P. data curation.

Acknowledgment—We thank Jaren Arbanas for providing enzyme characterization data.

References

1. Lowell, C. A. (2011) Src-family and Syk kinases in activating and inhibitory pathways in innate immune cells: signaling cross talk. *Cold Spring Harb. Perspect. Biol.* **3,** a002352 Medline
2. Kulathu, Y., Grothe, G., and Reth, M. (2009) Autoinhibition and adapter function of Syk. *Immunol. Rev.* **232,** 286–299 CrossRef Medline
3. Zhang, J., Billingsley, M. L., Kincaid, R. L., and Siraganian, R. P. (2000) Phosphorylation of Syk activation loop tyrosines is essential for Syk function: an *in vivo* study using a specific anti-Syk activation loop phosphotyrosine antibody. *J. Biol. Chem.* **275,** 35442–35447 CrossRef Medline
4. Couture, C., Williams, S., Gauthier, N., Tailor, P., and Mustelin, T. (1997) Role of Tyr518 and Tyr519 in the regulation of catalytic activity and substrate phosphorylation by Syk protein-tyrosine kinase. *Eur. J. Biochem.* **246,** 447–451 CrossRef Medline
5. Zhang, J., Kimura, T., and Siraganian, R. P. (1998) Mutations in the activation loop tyrosines of protein tyrosine kinase Syk abrogate intracellular signaling but not kinase activity. *J. Immunol.* **161,** 4366–4374 Medline
6. Furlong, M. T., Mahrenholz, A. M., Kim, K. H., Ashendel, C. L., Harrison, M. L., and Geahlen, R. L. (1997) Identification of the major sites of autophosphorylation of the murine protein-tyrosine kinase Syk. *Biochim. Biophys. Acta* **1355,** 177–190 CrossRef Medline
7. Sanderson, M. P., Wex, E., Kono, T., Uto, K., and Schnapp, A. (2010) Syk and Lyn mediate distinct Syk phosphorylation events in FcεRI-signal transduction: implications for regulation of IgE-mediated degranulation. *Mol. Immunol.* **48,** 171–178 CrossRef Medline
8. Keshvara, L. M., Isaacson, C. C., Yankee, T. M., Sarac, R., Harrison, M. L., and Geahlen, R. L. (1998) Syk- and Lyn-dependent phosphorylation of Syk on multiple tyrosines following B cell activation includes a site that negatively regulates signaling. *J. Immunol.* **161,** 5276–5283 Medline
9. Mocsai, A., Ruland, J., and Tybulewicz, V. L. (2010) The SYK tyrosine kinase: a crucial player in diverse biological functions. *Nat. Rev. Immunol.* **10,** 387–402 CrossRef Medline
10. Monroe, J. G. (2006) ITAM-mediated tonic signalling through pre-BCR and BCR complexes. *Nat. Rev. Immunol.* **6,** 283–294 CrossRef Medline
11. Geahlen, R. L. (2014) Getting Syk: spleen tyrosine kinase as a therapeutic target. *Trends Pharmacol. Sci.* **35,** 414–422 CrossRef Medline
12. Norman, P. (2014) Spleen tyrosine kinase inhibitors: a review of the patent literature 2010–2013. *Expert Opin. Ther. Pat.* **24,** 573–595 CrossRef Medline
13. Cha, H. S., Boyle, D. L., Inoue, T., Schoot, R., Tak, P. P., Pine, P., and Firestein, G. S. (2006) A novel spleen tyrosine kinase inhibitor blocks c-Jun N-terminal kinase-mediated gene expression in synoviocytes. *J. Pharmacol. Exp. Ther.* **317,** 571–578 CrossRef Medline
14. Bond, P. J., and Faraldo-Gómez, J. D. (2011) Molecular mechanism of selective recruitment of Syk kinases by the membrane antigen-receptor complex. *J. Biol. Chem.* **286,** 25872–25881 CrossRef Medline
15. Arias-Palomo, E., Recuero-Checa, M. A., Bustelo, X. R., and Llorca, O. (2009) Conformational rearrangements upon Syk auto-phosphorylation. *Biochim. Biophys. Acta* **1794,** 1211–1217 CrossRef Medline
16. Grädler, U., Schwarz, D., Dresing, V., Musil, D., Bomke, J., Frech, M., Greiner, H., Jäkel, S., Rysiok, T., Müller-Pompalla, D., and Wegener, A. (2013) Structural and biophysical characterization of the Syk activation switch. *J. Mol. Biol.* **425,** 309–333 CrossRef Medline
17. Yan, Q., Barros, T., Visperas, P. R., Deindl, S., Kadlecek, T. A., Weiss, A., and Kuriyan, J. (2013) Structural basis for activation of ZAP-70 by phosphorylation of the SH2-kinase linker. *Mol. Cell. Biol.* **33,** 2188–2201 CrossRef Medline
18. Tsang, E., Giannetti, A. M., Shaw, D., Dinh, M., Tse, J. K., Gandhi, S., Ho, H., Wang, S., Papp, E., and Bradshaw, J. M. (2008) Molecular mechanism of the Syk activation switch. *J. Biol. Chem.* **283,** 32650–32659 CrossRef Medline
19. Papp, E., Tse, J. K., Ho, H., Wang, S., Shaw, D., Lee, S., Barnett, J., Swinney, D. C., and Bradshaw, J. M. (2007) Steady state kinetics of spleen tyrosine kinase investigated by a real time fluorescence assay. *Biochemistry* **46,** 15103–15114 CrossRef Medline

20. Parker, M. W., Lo Bello, M., and Federici, G. (1990) Crystallization of glutathione *S*-transferase from human placenta. *J. Mol. Biol.* **213,** 221–222 CrossRef Medline
21. Narula, S. S., Yuan, R. W., Adams, S. E., Green, O. M., Green, J., Philips, T. B., Zydowsky, L. D., Botfield, M. C., Hatada, M., and Laird, E. R. (1995) Solution structure of the C-terminal SH2 domain of the human tyrosine kinase Syk complexed with a phosphotyrosine pentapeptide. *Structure* **3,** 1061–1073 CrossRef Medline
22. Fütterer, K., Wong, J., Grucza, R. A., Chan, A. C., and Waksman, G. (1998) Structural basis for Syk tyrosine kinase ubiquity in signal transduction pathways revealed by the crystal structure of its regulatory SH2 domains bound to a dually phosphorylated ITAM peptide. *J. Mol. Biol.* **281,** 523–537 CrossRef Medline
23. Zhang, Y., Oh, H., Burton, R. A., Burgner, J. W., Geahlen, R. L., and Post, C. B. (2008) Tyr130 phosphorylation triggers Syk release from antigen receptor by long-distance conformational uncoupling. *Proc. Natl. Acad. Sci. U.S.A.* **105,** 11760–11765 CrossRef Medline
24. Geahlen, R. L. (2009) Syk and pTyr'd: signaling through the B cell antigen receptor. *Biochim. Biophys. Acta* **1793,** 1115–1127 CrossRef Medline
25. Xu, Y., Harder, K. W., Huntington, N. D., Hibbs, M. L., and Tarlinton, D. M. (2005) Lyn tyrosine kinase: accentuating the positive and the negative. *Immunity* **22,** 9–18 CrossRef Medline
26. Dueber, J. E., Yeh, B. J., Chak, K., and Lim, W. A. (2003) Reprogramming control of an allosteric signaling switch through modular recombination. *Science* **301,** 1904–1908 CrossRef Medline
27. Antenucci, L., Hytönen, V. P., and Ylänne, J. (2018) Phosphorylated immunoreceptor tyrosine-based activation motifs and integrin cytoplasmic domains activate spleen tyrosine kinase via distinct mechanisms. *J. Biol. Chem.* **293,** 4591–4602 CrossRef Medline
28. Bohnenberger, H., Oellerich, T., Engelke, M., Hsiao, H. H., Urlaub, H., and Wienands, J. (2011) Complex phosphorylation dynamics control the composition of the Syk interactome in B cells. *Eur. J. Immunol.* **41,** 1550–1562 CrossRef Medline
29. Shults, M. D., Janes, K. A., Lauffenburger, D. A., and Imperiali, B. (2005) A multiplexed homogeneous fluorescence-based assay for protein kinase activity in cell lysates. *Nat. Methods* **2,** 277–283 CrossRef Medline
30. Meng, F., Wiener, M. C., Sachs, J. R., Burns, C., Verma, P., Paweletz, C. P., Mazur, M. T., Deyanova, E. G., Yates, N. A., and Hendrickson, R. C. (2007) Quantitative analysis of complex peptide mixtures using FTMS and differential mass spectrometry. *J. Am. Soc. Mass Spectrom.* **18,** 226–233 CrossRef Medline
31. Yates, J. R., 3rd, Morgan, S. F., Gatlin, C. L., Griffin, P. R., and Eng, J. K. (1998) Method to compare collision-induced dissociation spectra of peptides: potential for library searching and subtractive analysis. *Anal. Chem.* **70,** 3557–3565 CrossRef Medline
32. Chrestensen, C. A., Schroeder, M. J., Shabanowitz, J., Hunt, D. F., Pelo, J. W., Worthington, M. T., and Sturgill, T. W. (2004) MAPKAP kinase 2 phosphorylates tristetraprolin on *in vivo* sites including Ser178, a site required for 14-3-3 binding. *J. Biol. Chem.* **279,** 10176–10184 CrossRef Medline